

# A Multiple Hypothesis People Tracker for Teams of Mobile Robots

Nicolas A. Tsokas and Kostas J. Kyriakopoulos

**Abstract**—This paper tackles the problem of tracking walking people with multiple moving robots equipped with laser rangefinders. We present an adaptation to the classic Multiple Hypothesis Tracking method, which allows for one-to-many associations between targets and measurements in each cycle and is thus capable of operating in a multi-sensor scenario. In the context of two experiments, the successful integration of our tracking algorithm to a dual-robot setup is assessed.

## I. INTRODUCTION

Tracking walking people by mobile robots has been tackled in many ways and under different perspectives in the literature. As a problem, walking people tracking falls within the general scope of target tracking. However, in contrast to generic targets usually moving stochastically, human walking exhibits recurrent patterns both in the behavioural level, as people tend to follow specific paths ([1], [2]), and in the motion level, as human body makes specific stereotyped movements during walking ([3], [4]).

Methods for walking people tracking are mainly based on either cameras ([5], [6]), or laser rangefinders ([8], [9], [18]), or a combination of these two ([10], [7]). Collecting sensory data, and fusing data from multiple sensors ([11], [12]), is followed by either making simplifying assumptions about human walking ([13], [9]) or explicitly modeling leg-motion in order to detect people. Actual tracking is accomplished with the use of a data association method like Multiple Hypothesis Tracking (MHT) ([14], [9]) or other Probabilistic Data Association method usually with Kalman or Particle Filters ([6], [7]).

Tracking people by observing their legs by definition involves handling frequent occlusion circumstances due to the nature of human walking. In addition, as very often people tend to walk in groups of two or more persons, occluded legs and crossing trajectories become even more frequent. Accommodating occlusion in human walking is a good reason to use a group of robots instead of one robot alone ([11], [12]).

Algorithms presented in the literature for walking people tracking with laser rangefinders usually concern either a single moving robot, or a set of static sensors. This paper presents an algorithm that runs on a team of moving robots that communicate with a central monitoring station.

In [9] we proposed a walking person tracker for laser-equipped mobile robots based on Reid's Multiple Hypothesis Tracking (MHT) method ([15]), where the rangefinder scans

at the height of the legs. In this paper we present an extension to the MHT method which, unlike classic MHT, can fuse tracking data from different sensors. Our contribution is the adaptation of MHT so as to handle one-to-many associations between targets and measurements in each step. Based on the above we propose a people tracking algorithm, which runs in parallel on multiple moving robots and a central station.

The rest of the paper is structured as follows: section II outlines the main concepts of our tracking method operating on a single robot, section III describes the proposed extension to the MHT method and how it was used in a multi-robot context, section IV discusses the conducted experiments and results and section V draws the conclusion and reveals planned future work.

## II. OUTLINE OF THE TRACKING METHOD

Our method for people tracking can be roughly divided in the following parts.

### A. Data Filtering and Clustering

In the case of highly reflective or dark colored surfaces, laser scanners are often prone to false measurements. Data filtering considers scan points with range greater than 8 meters as outliers and eliminates them.

The scan is smoothed by employing a median filter and then scan points are grouped into clusters. Clusters denote sets of points which, due to their proximity, potentially belong to the same real world object. The criterion for clustering is the one introduced in [16] and extended in [17].

### B. Shape Extraction

The shapes of interest to our algorithm are: line segments, which help localization and background detection, and circle arcs, which can potentially be associated to human legs. The point groups formed by the clustering module are inspected for these types of shapes.

The inspection procedure is based on the Ramer (Douglas-Peucker) algorithm [19], according to which, for each cluster, the first and last points are connected by a straight line. For all remaining cluster points the distance to the line is calculated and if the maximum distance exceeds a given threshold, then the line is splitted in the point of the maximum distance and two new sets of points are created. The difference here is that emerging point sets, when they cannot be fit by a line segment, are checked against the possibility of representing a leg by fitting circle arcs of dimensions compatible to common anthropometric data.

Circle arcs assigned to human legs are used for object tracking. The set of measurements passed to the tracking

Nicolas A. Tsokas and Kostas J. Kyriakopoulos are with Control Systems Laboratory, School of Mechanical Engineering, National Technical University of Athens, Greece {tsokas@ekt.gr, kkyria@mail.ntua.gr}

procedure is formed by the centroids of the corresponding point sets. Centroids have been preferred over the centers of the corresponding circles, as the latter can yield large errors due to human clothing.

### C. Object Tracking

MHT has been implemented based on [15] with the difference that, as measurements represent clusters of 3 or more points and given the sensor resolution the probability of false alarms has been considered negligible. After all, in the unlikely case that a false alarm initiates an object, the latter will quickly be eliminated when the next sets of measurements get processed.

Human walking being relatively stable (usually 1.0 to 1.5m/s), and given the periodic motion of human legs, in the context of Kalman filtering their acceleration has been modelled as white noise. When a moving object, i.e. a leg candidate, is lost from sensor sight, a counter is initiated and the object is assigned the *occluded* status. The position of objects in occluded status is updated by using the estimated a priori position of the corresponding KF. When the occlusion counter reaches a predefined number of steps, the object is discarded.

### D. People Tracking

The people tracking module exploits the object tracking inference in order to calculate the trajectories of people walking by. The assumption involved here is that, during normal walking, the relative positions of the human center of gravity (CoG) and legs satisfy the following two arguments: a) the triangle defined by the human CoG and the feet tends to stay isosceles with its base parallel to the ground and b) the plane defined by that triangle is quasi-normal to the ground. This way a human is considered to be making less effort to keep their balance. These two arguments are valid for the scanning plane of the laser rangefinder as well, as the latter is normally parallel to the ground.

The people tracking algorithm maintains a Kalman Filter for every people detected. By combining this KF with the two KFs maintained by the Object Tracker for the two legs, the above assumption and some basic geometry, the People Tracker can accommodate for periods of occlusion of one or even of both legs. It can also identify a human even in the case when, due to occlusion, one or both legs have been mistakenly considered by the object tracking module as new objects and their trajectories have been reset.

## III. MULTI-ROBOT MULTIPLE HYPOTHESIS TRACKING

Multiple Hypothesis Tracking method, as usually implemented ([15], [14]), and as used in our presented algorithm above, applies to scenarios involving a single robot. Therefore, a basic rule of MHT is that, in each step, each target can only be associated with a single measurement. In this paper we propose a multi-robot MHT, in the context of which a pool is formed with measurements originating from all robots sensors and one-to-many relationships are allowed between

targets and measurements. Thus, supposing the team consists of  $n$  robots, up to  $n$  measurements can now be assigned to a single target, existing or new, provided they originate from different robots. The latter is the additional rule followed by the MHT algorithm during the association of measurements to possible targets.

With respect to selecting the dominant association hypotheses, extending the method to the multi-robot case requires the derivation of hypotheses probabilities to be adapted, so as to accommodate for measurements from multiple sensors with overlapping fields of view. In the following paragraphs a probability analysis for such a multi-robot setup is presented.

Following the notation of the related literature, let  $\Omega_j^k$  be the  $j$ -th hypothesis at time  $k$ , let  $\Omega_{p(j)}^{k-1}$  be its parent hypothesis and let  $\Psi_j(k)$  denote a set of assignments that associates the measurements at time  $k$ , namely  $Z_k$ , to either existing or new targets. The set  $\Psi_j(k)$  is combined with  $\Omega_{p(j)}^{k-1}$  and so  $\Omega_j^k$  emerges.

The probability of the child hypothesis  $\Omega_j^k$  can be calculated recursively if the probability of its parent  $\Omega_{p(j)}^{k-1}$  and the probability of the assignment set  $\Psi_j(k)$  are known [15]:

$$P(\Omega_j^k | Z_k) = P(\Psi_j(k), \Omega_{p(j)}^{k-1} | Z_k) = c \cdot P(Z_k | \Psi_j(k), \Omega_{p(j)}^{k-1}) \cdot P(\Psi_j(k) | \Omega_{p(j)}^{k-1}) \cdot P(\Omega_{p(j)}^{k-1}) \quad (1)$$

The rightmost term in 1 is the recursive term, i.e. the probability of the parent hypothesis which is known from the previous iteration, whereas  $c$  is a normalizer. The leftmost term after the normalizer is the likelihood of the measurement set  $Z_k$  given the specific association hypothesis. Finally, the central term is the probability of the assignment of measurements to targets, given only the parent hypothesis and if no real knowledge on the actual measurement positions is implied.

### A. Definitions and Assumptions

As stated earlier we do not consider false alarms, as measurements emerge from fusing sets of scan points. Likewise, for a given robot the probability of detection is 1.0 for all targets lying within its field of view. We further assume that the team consists of identical robots with identical sensors, in this case laser rangefinders.

We define  $N$  as the number of existing targets, i.e. targets whose existence is implied by the parent hypothesis.  $M^k$  denotes the size of the current measurement set  $Z_k$ ,  $M_D^k$  will hence denote the number of measurements of the current measurement set that are associated with existing targets and  $M_N^k$  the number of those measurements associated to new targets. In the context of this paper we stick with Reid's notation for the MHT part, so further track statuses, like *occluded* and *deleted* ([14]) are only considered in a later stage of the algorithm. Therefore, under our assumptions, it holds:

$$M^k = M_D^k + M_N^k \quad (2)$$

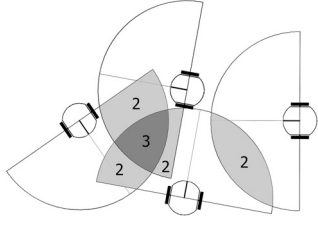


Fig. 1. Overlapping fields of view. Light grey (2) areas are concurrently monitored by 2 robots, dark grey (3) areas by 3 robots.

which means that in each step measurements originate from either existing or new targets.

As robots move the fields of view of their sensors often overlap. There are areas sensed by a single robot and areas viewed by two or more robots simultaneously as illustrated in Fig. 1. Let  $E_i^k$  be the total area simultaneously monitored by exactly  $i$  robots at time  $k$ . With respect to Fig. 1, for example,  $E_2^k$  is defined as the sum of all areas denoted by "2". We define  $E_{ef}^k$  as the total area effectively sensed by the system, thus it holds  $E_{ef}^k = \sum_{i=1}^n E_i^k$ , where  $n$  the number of team robots.  $k$  will hence be dropped for simplicity.

With respect to the above, we define  $N_{D_i}$  as the number of existing targets, i.e. targets implied by the parent hypothesis, concurrently detected by  $i$  robots. As the probability of detection is 1.0,  $N_{D_i}$  is equal to the number of existing targets lying in area  $E_i$ . The total number of existing targets detected will be denoted by  $N_D = \sum_{i=1}^n N_{D_i}$ .

We further define  $N_{N_i}$  as the number of new targets concurrently detected by exactly  $i$  robots.  $N_N$  denotes the total number of new targets detected by the system at time  $k$  according to the assignment hypothesis in question and it holds  $N_N = \sum_{i=1}^n N_{N_i}$ .

Further, according to the above assumptions, the numbers of measurements and the numbers of targets are connected with the following relationships:

$$M_{D_i} = iN_{D_i} \Rightarrow M_D = \sum_{i=1}^n iN_{D_i} \quad (3)$$

$$M_{N_i} = iN_{N_i} \Rightarrow M_N = \sum_{i=1}^n iN_{N_i} \quad (4)$$

where  $M_{D_i}$  represents the number of measurements at time  $k$  assigned to existing targets within the areas concurrently monitored by  $i$  robots and  $M_{N_i}$  represents the number of measurements assigned to new targets within those areas.

### B. Likelihood of Measurements

We assume that a target associated with a measurement  $Z_k^i$  has a Gaussian probability distribution centered around the measurement prediction. We define variable  $\delta_i$  as being 1 if measurement  $Z_k^i$  has been associated to an existing target, 0 otherwise.  $\mathcal{N}_{Z_i}$  denotes the Gaussian distribution corresponding to the track of the target (if any) associated

with the measurement  $Z_k^i$ . We further define variable  $\zeta_i$  as 1 if measurement  $Z_k^i$  is assigned to a new target that has already been initiated by another robot's measurement, 0 otherwise, such that  $\sum_{i=1}^{M^k} \zeta_i + N_N = M_N$ .  $\mathcal{N}_s$  denotes a Gaussian distribution corresponding to the sensor accuracy, which describes the probability that a robot detects an object at the neighborhood of an already detected target. If the pdf of a new target emerging somewhere within the sensed area is considered uniform, the corresponding probability is denoted by  $1/E_{ef}$ . Thus, the likelihood of measurements, given the parent hypothesis and the measurements-to-targets association is expressed as follows:

$$P(Z_k | \Psi_j(k), \Omega_{p(j)}^{k-1}) = \frac{1}{E_{ef}^{N_N}} \prod_{i=1}^{M^k} \mathcal{N}_{Z_i}(Z_k^i)^{\delta_i} \mathcal{N}_s(Z_k^i)^{\zeta_i} \quad (5)$$

### C. Hypothesis Probability

As there are many possible combinations when assigning measurements to existing and new targets, there are many possible association sets  $\Psi_j(k)$ , each one having a probability related to that of the corresponding assignments. Following we derive the probability of the emerging hypotheses.

In Reid's analysis [15] it is assumed that the number of existing targets that are detected is given by a binomial distribution, whereas the number of new targets follows a Poisson distribution. Having assumed probability of detection equal to 1.0, the probability of numbers  $N_D$  and  $N_N$ , given the parent hypothesis  $\Omega_{p(j)}^{k-1}$ , will only depend on the probability of new targets, which is considered to follow a Poisson distribution, and the probability of targets coming out of the total sensed area, or deleted tracks, denoted by  $N - N_D$ , which follow a binomial distribution with probability of deletion equal to  $P_x$ :

$$P(N_D, N_N | \Omega_{p(j)}^{k-1}) = \frac{\beta_N^{N_N} E_{ef}^{N_N} \cdot e^{-\beta_N E_{ef}}}{N_N!} \cdot \frac{N! \cdot P_x^{(N-N_D)} (1-P_x)^{N_D}}{(N-N_D)! N_D!} \quad (6)$$

where the first fraction corresponds to the Poisson distribution,  $\beta_N$  being the density of new targets.

The probability of a specific assignment of measurements to targets is determined as 1 over the number of possible combinations satisfying Eq. 2. The number of possible such configurations is:

$$\begin{aligned} & \binom{M^k}{M_{D_1}} \cdot \binom{M^k - M_{D_1}}{M_{D_2}} \cdots \binom{M^k - \sum_{i=1}^{n-1} M_{D_i}}{M_{D_n}} \\ & \binom{M^k - \sum_{i=1}^n M_{D_i}}{M_{N_1}} \cdots \binom{M^k - \sum_{i=1}^n M_{D_i} - \sum_{i=1}^{n-1} M_{N_i}}{M_{N_n}} = \\ & = \frac{M^k!}{\prod_{i=1}^n M_{D_i}! M_{N_i}!} \stackrel{(3),(4)}{=} \frac{M^k!}{\prod_{i=1}^n (iN_{D_i})! (iN_{N_i})!} \quad (7) \end{aligned}$$

Therefore the corresponding probability is:

$$P(\text{configuration}|N_D, N_N) = \frac{\prod_{i=1}^n (iN_{D_i})!(iN_{N_i})!}{M^k!} \quad (8)$$

For a given configuration, there are many ways to assign the  $N_D$  detected targets to the  $N$  existing targets. The number of possible assignments is given by  $\frac{N!}{(N-N_D)!}$ .

And the corresponding probability is:

$$P(\text{assignment}|\text{configuration}) = \frac{(N - N_D)!}{N!} \quad (9)$$

Finally, the probability of the assignment of measurements to targets given only the parent hypothesis is the product of Equations 6, 8 and 9:

The probability of the child hypothesis  $\Omega_j^k$  can now be expressed by the following formula, where many terms, including the exponentiated effectively sensed area  $E_{ef}^{N_N}$ , have been canceled out and where  $c'$  incorporates all terms that do not depend on the choice of the assignment hypothesis (like  $M^k!$ ,  $E_{ef}$  etc.):

$$P(\Omega_j^k|Z_k) = P(\Omega_{p(j)}^{k-1}) \cdot c' \cdot \left[ \prod_{i=1}^{M^k} \mathcal{N}_{Z_i}(Z_k^i)^{\delta_i} \mathcal{N}_s(Z_k^i)^{\zeta_i} \right] \cdot \frac{\beta_N^{N_N} P_x^{(N-N_D)} (1 - P_x)^{N_D}}{N_N! N_D!} \cdot \left[ \prod_{i=1}^n (iN_{D_i})!(iN_{N_i})! \right] \quad (10)$$

which is the equation we propose to be used throughout the hypothesis selection procedure.

Once the dominant hypotheses have been nominated, the position of each target is calculated by merging all the two-dimensional Gaussian distributions, which correspond to the measurements assigned to each target.

#### D. System Overview

The tracking algorithm is divided in two parts, one implemented onboard the robots, identical on each of them, and the other functioning on a desktop computer, hence called central station. Reliable communication between the system components is assumed.

Robot side, scan points received from the local laser rangefinder are processed up to the point when actual moving or static objects are extracted through the locally implemented MHT-based data association module. Information on objects position provided by the local Object Tracker reflects the robot's individual view of the environment and, although referring to the global coordinate system of the map, it corresponds to the time when the local rangefinder carried out the measurement. A synchronization module undertakes the conversion of locally tracked object positions to the time point requested by the central station.

The central station requests object positions with a constant frequency (e.g. every  $250ms$  or  $4Hz$  frequency), whereas on each robot scans are assigned a timestamp denoting the global time they were acquired. Given that the local Object Trackers associate measurement data to tracked

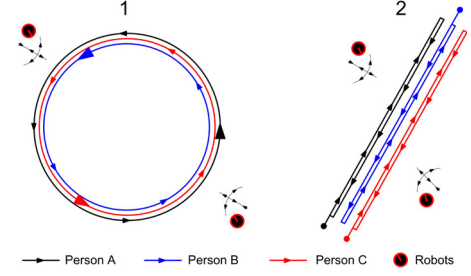


Fig. 2. Paths followed by the walking persons and the robots during the two experiments (1 and 2).

objects, the synchronization module can interpolate object positions to the exact time requested by the central station.

Data association information is not forwarded to the central station. The latter, through the global object tracking module, performs a separate data association using the multi-robot MHT method presented in Section III.

#### IV. EXPERIMENTAL EVALUATION

The presented method was tested in the context of two experiments involving two moving robots and three walking persons, whose paths followed are depicted in Fig. 2. Robots followed a repeated pre-programmed moving pattern at a speed of  $20cm/s$ , which attempted to approximate the movement style of a service robot within a populated area. Ground truth was provided by camera mounted on a bridge crane at a height of  $8,5m$  over the experiments area.

The data collected during the experiments were processed by two versions of the tracking algorithm: a single-robot version, considering data recorded by one of the robots and a dual-robot version, based on the proposed extended MHT algorithm and considering data from both robots.

It should be stressed that the recorded positions concern each time the dominant MHT hypothesis (set of associations between measurements and targets), in other words the branch of the MHT hypotheses tree with the highest probability, which might change at a later stage as more than one hypotheses survived from one processing cycle to the next. With respect mainly to the single-robot case, such hypothesis switches are visible in resulting graphs in the form of sharp path changes: due to extensive occlusion the algorithm temporarily misses the actual path of the tracked person, however the path is corrected based on later data.

##### A. First Experiment

The first experiment involved three persons walking in circles in front of the robots as depicted in Fig. 2, part 1. Due to its pattern, the movement of the walking persons yielded multiple instances of occlusion, however each person was each time clearly seen by at least one robot.

With reference to Fig. 3, the path produced for person A (similar for B and C) when the algorithm ran on one robot is reflected on the left graph. Circle-shaped signs following the lines coming out of the path (Fig. 3, left graph) denote instances when person A was occluded by another person

with reference to the measuring robot. As mentioned in the algorithm overview, during that period the Kalman Filter assigned to person A, in lack of a real observation, was being updated with its own a priori estimated position.

With reference to the right graph of Fig. 3, the dual-robot version of the algorithm clearly produces a much more accurate path for the person tracked as successive occlusions are compensated by the presence of two measuring robots.

### B. Second Experiment

The second experiment intended to reveal the advantage of the multi-robot version of the algorithm over the single-robot version in a circumstance frequently observed when people walk in groups. The experiment involved two persons, A and C, walking in front of the robots the one next to the other as illustrated in Fig. 2, part 2. The third person followed the opposite path direction. The paths followed by A and C were parallel, the distance between the two being approximately 80cm. Due to the latter fact there were moments when two legs of two different persons were closer than the legs of a single walking person. In addition, the algorithm had to accommodate for the continuous occlusions of the legs. The paths produced by the two versions of the algorithm are depicted in Figures 4, 5 and 6.

The single-robot version, which was run on the upper-left robot with respect to 2, exhibited no difficulty to follow person A in real-time as the latter was clearly seen by the robot all the way.

Concerning person B, the algorithm eventually produced a consistent track, in terms that it did not get confused about the number of persons and also kept a continued track for the person's path from the beginning to the end. However, a difficulty of the single-robot version, to follow the tracked person in real-time in occlusion circumstances is implied in Fig. 5. As for person C, the single-robot version of the algorithm failed to produce a continuous path and the corresponding track was stopped several times. Tracking was eventually re-established, but different persons were implied. This is because, due to occlusion, person C repeatedly remained out of robot sight for longer than the algorithm could handle.

In contrast, the dual-robot version of the algorithm successfully tracked all three persons, as it used scan data from two different perspectives, thus practically eliminating legs occlusion.

### C. Single-robot vs dual-robot algorithm

Table I illustrates the mean values of the offsets of the paths measured by the existing single-robot tracker and the multi-robot tracking algorithm, which is based on the proposed extension of the classic MHT method. With respect to the former, and in order for a comparison to be meaningful, for the track that was mistakenly split in parts, offset values in the table refer to the corresponding combined paths.

Values measured for the multi-robot algorithm denote an improvement varying from 26% to 66%. Although offset values are not suitable for an absolute assessment of the

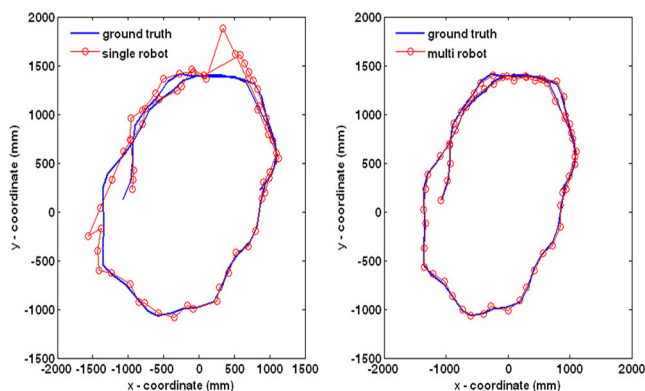


Fig. 3. First experiment. Person A. Left graph refers to the single-robot, right graph refers to the multi-robot version.

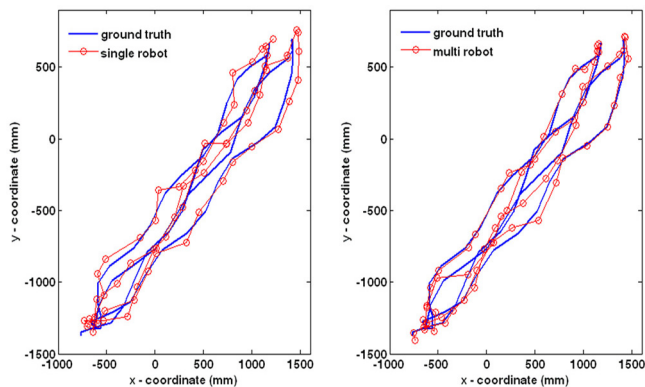


Fig. 4. Second experiment. Person A. Left graph refers to the single-robot, right graph refers to the multi-robot version.

algorithm, as they are subject to robots localization errors, the difference in accuracy between the paths produced by the single-robot and the multi-robot methods is significant. Equally important is the improvement in the capability of the system to discern walking legs and to disambiguate observed objects in occlusion circumstances.

## V. CONCLUSIONS AND FUTURE WORK

This paper presented an algorithm for tracking walking people suitable for systems comprising a team of multiple moving robots and a central station. An extension to the classic Multiple Hypothesis Tracking method was presented, which can handle measurements coming from multiple sensors. The main contribution of this paper is the probability analysis for the multi-sensor MHT method, resulting in Eq. 10, which is used throughout the hypothesis selection procedure. The proposed method was evaluated in two experiments involving two moving robots and three walking persons.

### A. Conclusions

The conducted experiments revealed that, when changing from the single-robot to the multi-robot algorithm, there is a significant improvement of the paths calculated for the tracked walking people. In addition the experiments revealed that, in circumstances where people walk close to each other,



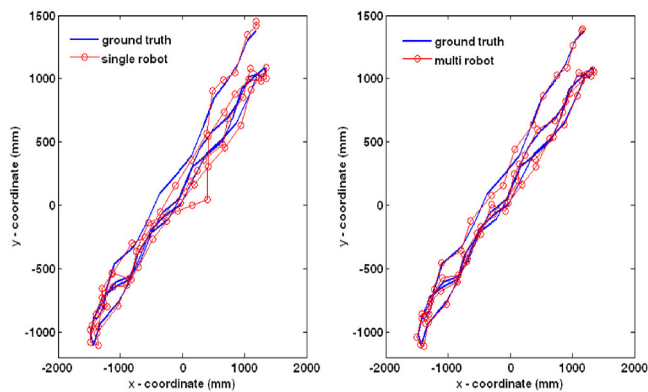


Fig. 5. Second experiment. Person B. Left graph refers to the single-robot, right graph refers to the multi-robot version.

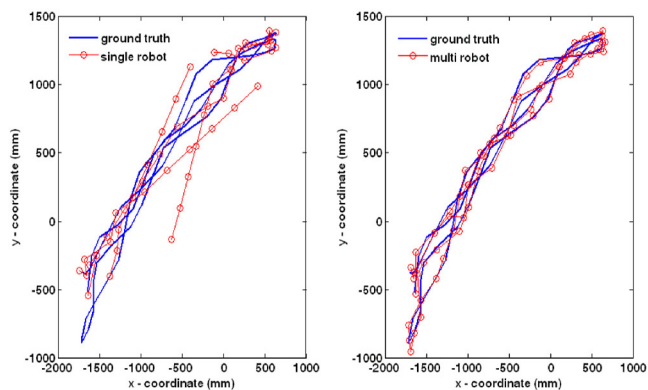


Fig. 6. Second experiment. Person C. Left graph refers to the single-robot, right graph refers to the multi-robot version.

there are cases when only the multi-robot version of the algorithm can successfully track the occluded persons.

### B. Future Work

We are currently enhancing the proposed algorithm by adapting the multi-robot MHT implementation so as to handle situations where the probability of detection is lower than 1.0. The latter, by invalidating Eq. 3 and 4, involves a thorough probability analysis for the assignment of measurements to targets where a target in a  $E_i$  area could potentially be tracked by 0 up to  $i$  robots.

The proposed method for multi-robot walking person tracking will soon be tested and evaluated in the context of an experiment of a larger scale. Its effectiveness will be assessed in a more demanding out-of-laboratory environment.

Our efforts and interest are directed towards implementing a completely decentralized approach, in the context of which each robot will be running its own global object and people tracker, much like in the single-robot case, but this time sharing object tracking information with the other team robots in real-time.

### REFERENCES

[1] G. Cielniak, M. Bennewitz and W. Burgard, "Robust localization of persons based on learned motion patterns", *In Proc. of the European Conference on Mobile Robots (ECMR)*, 2003.

TABLE I  
MEAN OFFSETS OF THE CALCULATED PATHS

	Single – robot	Multi – robot	Diff.
Exp. 1, person A	82.7 mm	27.9 mm	-66%
Exp. 2, person A	61.6 mm	45.5 mm	-26%
Exp. 2, person B	123.9 mm	59 mm	-52%
Exp. 2, person C	78.7 mm	43.2 mm	-45%

[2] A. Bruce and G. Gordon, "Better motion prediction for people tracking", *In Proc. of the International Conference on Robotics and Automation (ICRA)*, New Orleans, USA, 2004.

[3] G. Taylor and L. Kleeman, "A Multiple Hypothesis Walking Person Tracker with Switched Dynamic Model", *Proceedings of the Australasian Conference on Robotics and Automation*, Australia, 2004.

[4] J. Cui, H. Zha, H. Zhao and R. Shibusaki, "Laser-based Interacting People Tracking Using Multi-level Observations", *Proceedings of the 2006 IEEE/RSJ Int. Conf. on Intelligent Robots and Systems*, Beijing, China, 2006.

[5] F. Fleuret, J. Berclaz, R. Lengagne and P. Fua, "Multi-Camera People Tracking with a Probabilistic Occupancy Map", *IEEE Transactions on Pattern Analysis and Machine Intelligence*, Vol. 30, Nr. 2, pp. 267 - 282, February 2008.

[6] D. Schulz, W. Burgard, D. Fox, A. B. Cremers, "Tracking Multiple Moving Objects with a Mobile Robot", *IEEE Computer Society Conference on Computer Vision and Pattern Recognition (CVPR'01)*, vol. 1, pp. 371-377, 2001.

[7] M. Kobilarov, J. Hyams, P. Batavia and G. S. Sukhatme, "People tracking and following with mobile robot using an omnidirectional camera and a laser", *In IEEE International Conference on Robotics and Automation*, pp. 557-562, 2006.

[8] K.O. Arras, O.M. Mozos and W. Burgard, "Using Boosted Features for the Detection of People in 2D Range Data", *IEEE International Conference on Robotics and Automation*, pp. 3402-3407, Rome, Italy, 2007.

[9] N. Tsokas, K. Kyriakopoulos, "A Multiple Walking Person Tracker for Laser-Equipped Mobile Robots", *Proceedings of the 10th Conference on Intelligent Autonomous Systems*, Baden-Baden, Germany, 2008.

[10] J. Cui, H. Zha, H. Zhao and R. Shibusaki, "Multi-Modal Tracking of People Using Laser Scanners and Video Camera", *Image and Vision Computing*, v.26 n.2, p.240-252, February, 2008

[11] K. Iwata, K. Nakamura, H. Zhao, R. Shibusaki, H. Takeuchi, "Object detection with background occlusion modeling by using multiple laser range scanners", *Proceedings of the 6th International Conference on ASIA GIS*, 2006.

[12] H. Zhao, Y. Chen, X. Shao, K. Katabira and R. Shibusaki, "Monitoring a populated environment using single-row laser range scanners from a mobile platform", *IEEE International Conference on Robotics and Automation*, pp. 4739-4745, Rome, Italy, 2007.

[13] E. Prassler, J. Scholz and E. Elfes, "Tracking People in a Railway Station During Rush-Hour", *Proc. of 1st Int. Conf. on Computer Vision Systems*, pp. 162179, Gran Canaria, Spain, 1999.

[14] K.O. Arras, S. Grzonka, M. Luber and W. Burgard, "Efficient People Tracking in Laser Range Data using a Multi-Hypothesis Leg-Tracker with Adaptive Occlusion Probabilities", *IEEE International Conference on Robotics and Automation*, Pasadena, CA, USA, 2008.

[15] D. B. Reid, "An Algorithm for Tracking Multiple Targets", *IEEE Transactions on Automatic Control*, AC-24(6):843-854, 1979.

[16] K. C. J. Dietmayer, J. Sparbert and D. Streller, "Model Based Object Classification and Object Tracking in Traffic Scenes", *IEEE Intelligent Vehicle Symposium*, Tokyo, Japan, pp. 2530, 2001.

[17] A. Mendes, L. Conde Bento and U. Nunes, "Multi-target Detection and Tracking with a Laserscanner", *IEEE Intelligent Vehicles Symposium*, University of Parma, Parma, Italy, June 14-17, 2004.

[18] A. Carballo, A. Ohya and S. Yuta, "Multiple People Detection from a Mobile Robot using Double Layered Laser Range Finders", *Workshop on People Detection and Tracking*, Kobe, Japan, May 2009

[19] U. Ramer, "An iterative procedure for the polygonal approximation of plane curves", *Computer Graphics and Image Processing*, 1(2), 244-256 (1972)